J. Opt. A: Pure Appl. Opt. **11** (2009) 114024 (5pp) doi:10.1088/1464-4258/11/11/114024

Rigorous analysis of vectorial plasmonic diffraction: single- and double-slit experiments

Pavel Ginzburg, Eitan Hirshberg and Meir Orenstein

EE Department, Technion, Haifa 32000, Israel

E-mail: gpasha@tx.technion.ac.il

Received 20 February 2009, accepted for publication 15 May 2009
Published 17 September 2009
Online at stacks.iop.org/JOptA/11/114024

Abstract
A rigorous vectorial formulation of the surface diffractive optics of plasmon polaritons is derived using the Green's function formalism. Theoretical predictions for several 2D plasmonic scenarios, i.e. plasmonic single-and double-slit diffraction, are exemplified and compared with published experimental observations. The importance, in near field diffraction, of all vectorial components of plasmonic modes is discussed.

Keywords: surface plasmon, diffraction, optics on a surface

(Some figures in this article are in colour only in the electronic version)

1. Introduction

Electromagnetic waves propagating on the interface between metal and dielectric substances—surface plasmon polaritons (SPP) [1]—have attracted a lot of scientific and technological interest in recent decades [2]. SPP are confined to the interface, and, under some circumstances, open up possibilities for sub-wavelength and even nano-confinement of visible and infra-red optical power [3, 4], overcoming the conventional diffraction limit [5, 6]. Complex waveguides [7–10] and cavities [11], based on the plasmonic effect, are promising candidates for incorporation into optical nano-circuitry. Two-dimensional (2D) nano-optics [12, 13] based on a single metal–dielectric interface may be important for sensing and lab-on-a-chip schemes where plasmon optics will interact with substances. Two-dimensional optics using plasmonics was exhibited experimentally—in 2D plasmonic focusing [14–16], as well as double-slit experiments [17]. The related field of SPP assisted extraordinary transmission [18] may be employed as an efficient nano-device for optical filtering and focusing [19]. Scattering of SPP by surface imperfections was investigated in [20], tailoring both far and near field behavior of out of plane scattered waves; however, surface (in plane) diffraction was not considered in detail.

In many cases diffraction scenarios are treated using a scalar model. This model asserts that each vector component of the electrical field diffracts independently of the other components. For plasmons, which are essentially TM waves, there is a strong coupling between the vector components. Furthermore, in the metal the main component is the longitudinal one. We dwell here on a vectorial solution to the diffraction problem. First, we analyze a plasmonic point source on the metal/dielectric interface, namely a 2D point source where the transverse direction (out of plane) is obtained by the eigenfunction of the plasmonic solution. The result is shown to converge into a plasmonic traveling wave when moving on the surface away from the source ('far field'). This point source is used to create a Green's function for the Rayleigh–Sommerfeld formalism [21] which will be employed to solve the diffraction scenarios. To emphasize, plasmonic point sources (dipole-like patterns) were investigated theoretically [22] and even experimentally [16]. However, similar to the polarization-independent pure spherical waves (not Hertz dipole patterns) that are of use in 3D diffraction related problems, the polarization-independent basis of SPPs is much more suitable. Here, we investigate such a point source and further employ it to the description of single- and double-slit diffraction and interference.

2. SPP point source

A plasmonic point source is located on the interface between dielectric and metal semi-infinite spaces (figure 1(a)). The basic plasmonic field is bounded to the surface, decaying

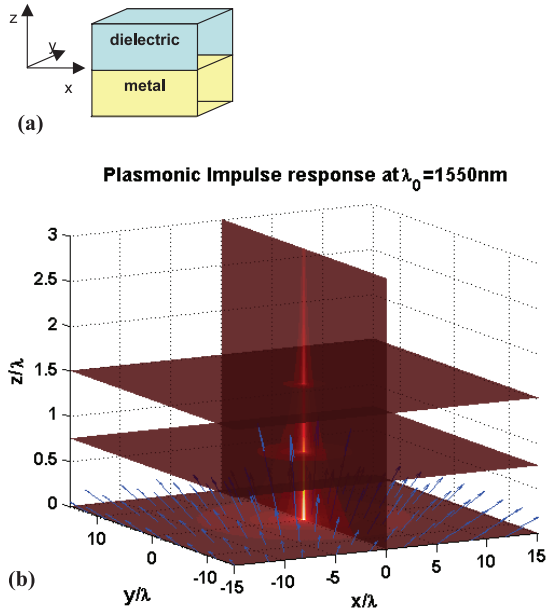

Figure 1. The SPP point source. (a) Dielectric/metal interface with coordinate system. (b) Electric field intensity of the SPP point source. The arrows indicate the polarization.

exponentially into both media. The SPP mode on each semi-infinite side of the metal–dielectric interface ($z = 0$) may be regarded as traveling in a 2D homogeneous medium, described by the proper Maxwell's wave equation. Employing azimuthal symmetry of cylindrical coordinates, only the z-component of the fields satisfies the 3D Helmholtz equation:

$$\nabla^2 E_z + \varepsilon_{\mathrm{d,m}} k_0^2 E_z = 0 \tag{1}$$

where ε_{d} and ε_{m} are the permittivities of the dielectric and metal material, respectively, and k_0 is the wavenumber in free space. Forcing an exponential decay when moving away from the surface ($|z| > 0$) reduces the equation to a 2D equation:

$$\nabla_t^2 E_z + k_\rho^2 E_z = 0 \tag{2}$$

with the following relations:

$$\begin{aligned} k_{z,\mathrm{d}} &= \sqrt{k_\rho^2 - \varepsilon_{\mathrm{d}} k_0^2} \\ k_{z,\mathrm{m}} &= -\sqrt{k_\rho^2 - \varepsilon_{\mathrm{m}} k_0^2}. \end{aligned} \tag{3}$$

The appropriate Green's function for this equation, with spatial delta excitation at the surface origin, is a zero-order Hankel function of the first kind, having a far field approximation of a cylindrical wave traveling away from the origin (assuming $\mathrm{e}^{-\mathrm{i}\omega t}$ time dependency). The other vector components of the magnetic and electric fields may be derived using Maxwell's equations on both sides of the interface. Imposing the boundary conditions we obtain:

$$\begin{aligned} \vec{E} = E_0 &\left(H_0^{(1)}(k_\rho \rho)\hat{z} - \frac{k_{zd}}{k_\rho} H_1^{(1)}(k_\rho \rho)\hat{\rho} \right) \\ &\times \exp(-k_{zd} z), \qquad z > 0 \end{aligned}$$

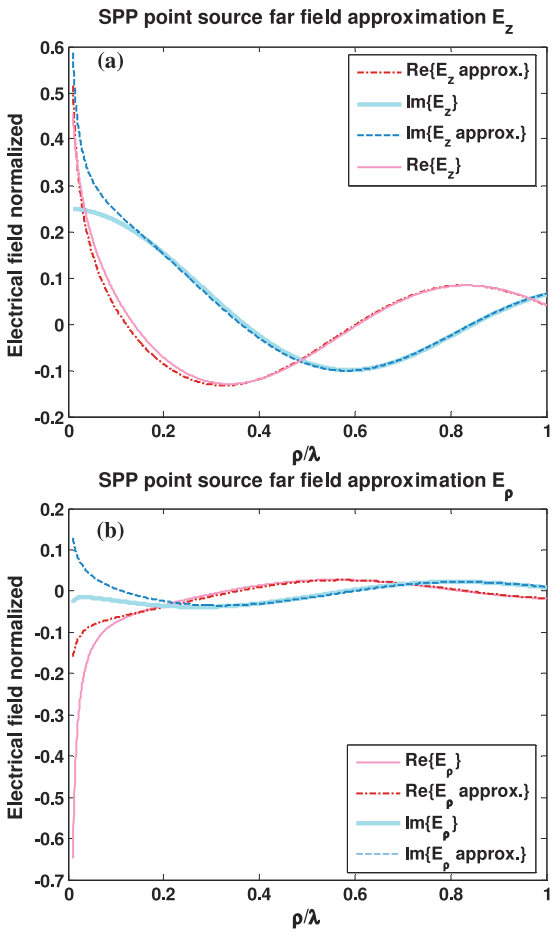

Figure 2. Electrical field of the SPP point source and its approximation by a cylindrical wave: (a) perpendicular (to surface) component; (b) parallel (to surface) component.

$$\begin{aligned} \vec{E}_0 &\left(H_0^{(1)}(k_\rho \rho)\hat{z} - \frac{k_{zm}}{k_\rho} H_1^{(1)}(k_\rho \rho)\hat{\rho} \right) \\ &\times \exp(-k_{zm} z), \qquad z \leqslant 0 \end{aligned} \tag{4}$$

with the known SPP dispersion relation

$$k_\rho = k_0 \sqrt{\frac{\varepsilon_{\mathrm{d}} \varepsilon_{\mathrm{m}}}{\varepsilon_{\mathrm{m}} + \varepsilon_{\mathrm{d}}}}. \tag{5}$$

The resulting field is depicted in figure 1(b)—the SPP indeed behaves as a cylindrical traveling wave. Asymptotic expansion of the Hankel functions results in the metal side:

$$\vec{E}_{\mathrm{m}} = \tilde{E}_0 \left(\hat{z} + \mathrm{i} \frac{k_{zm}}{k_\rho} \hat{\rho} \right) \exp(-k_{zm} z + \mathrm{i} k_\rho \rho). \tag{6}$$

This 'far field' approximation is valid as close as 0.3 free-space wavelengths away from the origin (figure 2).

3. SPP diffraction

A basic plasmonic diffraction problem is of a single slit in an opaque screen on the metal dielectric layer. The solution,

using the Rayleigh–Sommerfeld formalism, requires a Green's function which vanishes on the screen. The field components are strictly related via Maxwell's equation; specifically, the knowledge of z-component provides the possibility of evaluation of all the others. If the SPP retains its characteristics during the propagation, the diffraction of the z-component of the electric field will provide complete knowledge of the mode behavior.

The Green's function of the problem is the linear combination of the required component of the SPP point source, the sum of a point source, and its mirror image across the screen ($x = 0$) with opposite phase, namely the first Rayleigh–Sommerfeld solution:

$$\begin{aligned} G(\vec{\rho}, \vec{\rho}') &= -\frac{\mathrm{i}}{4} H_0^{(1)}(k_\rho \mathrm{P}) + \frac{\mathrm{i}}{4} H_0^{(1)}(k_\rho \tilde{\mathrm{P}}) \\ \mathrm{P}(x, y, y') &= \sqrt{(x - x')^2 + (y - y')^2} \\ \tilde{\mathrm{P}}(x, y, y') &= \sqrt{(x + x')^2 + (y - y')^2}. \end{aligned} \tag{7}$$

The formalism then allows evaluation of the diffraction pattern with the integral form:

$$\begin{aligned} E_z &= -\frac{\mathrm{i}}{2} k_\rho \int_{-\infty}^{\infty} E_{z,\mathrm{incident}} \frac{x}{\mathrm{P}(y')} H_1^{(1)}(k_\rho \mathrm{P}(y'))\, \mathrm{d}y' \\ E_x &= \frac{1}{2} \frac{k_z}{k_\rho} \int_{-\infty}^{\infty} E_{z,\mathrm{incident}} \frac{x^2}{\mathrm{P}^2(y')} \left(\frac{2}{\mathrm{P}(y')} H_1^{(1)}(k_\rho \mathrm{P}(y')) \right. \\ &\quad \left. - k_\rho H_0^{(1)}(k_\rho \mathrm{P}(y')) \right) \mathrm{d}y' \\ E_y &= \frac{1}{2} \frac{k_z}{k_\rho} \int_{-\infty}^{\infty} E_{z,\mathrm{incident}} \frac{x(y - y')}{\mathrm{P}^2(y')} \left(\frac{2}{\mathrm{P}(y')} H_1^{(1)}(k_\rho \mathrm{P}(y')) \right. \\ &\quad \left. - k_\rho H_0^{(1)}(k_\rho \mathrm{P}(y')) \right) \mathrm{d}y' \end{aligned} \tag{8}$$

where $E_{z,\mathrm{incident}}$ is the z-component of the incident SPP field. Here we consider the field amplitudes on the metal/dielectric surface, where they are maximal.

To emphasize, this technique approximates the field in the slit to be exactly the same as that of the incident field, which is a good approximation for slit dimensions wider than the wavelength. For a sub-wavelength slit, the interference between the plasmonic waves propagating in the slit plane will be significant.

4. Single slit diffraction and SPP Young's experiment

These equations (equations (8)) were employed to solve the SPP diffraction from a single slit. The slit width was taken to be four free-space wavelengths (4×1.55 μm). The diffraction pattern for the 'far' field is depicted in figure 3(a), and that for the 'near' field in figure 3(b). It may be seen that after the propagation of tens of free-space wavelengths the intensity pattern behaves like a free-space pattern of cylindrical waves. Figures 3(c) and (d) demonstrate the diffraction of the longitudinal E_y component, which does not exist in the incident wave. This component, inherent in the vectorial nature of the SPP, comprises higher

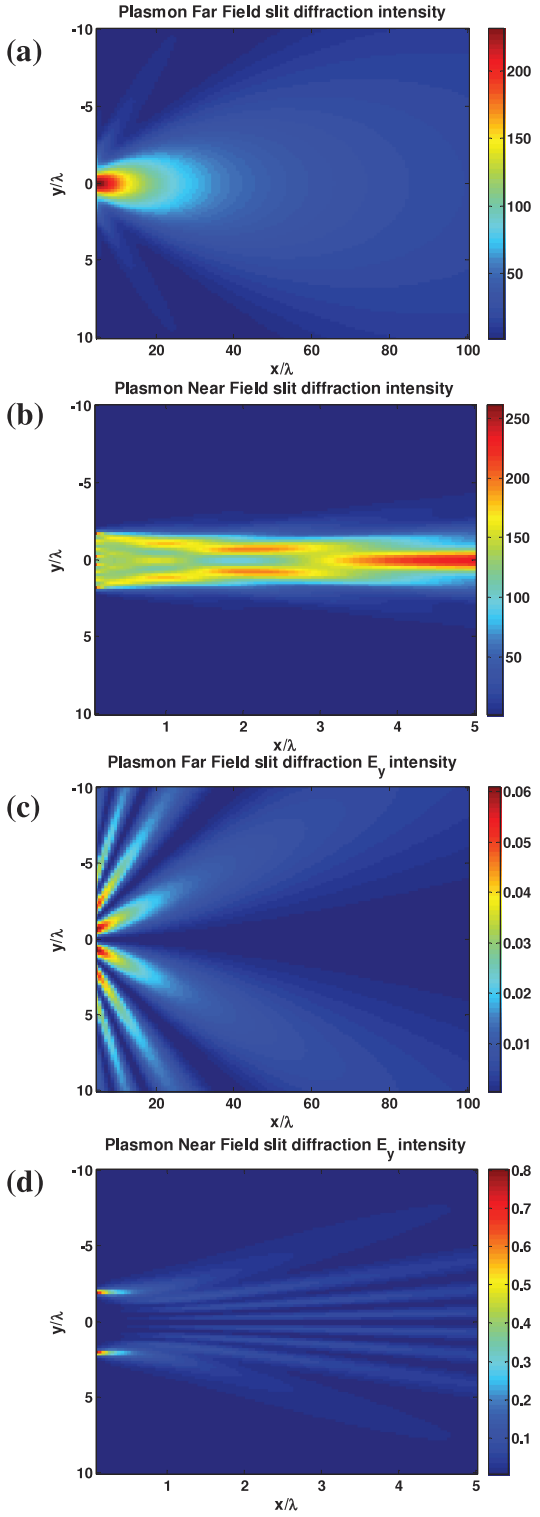

Figure 3. Single (4λ) slit SPP diffraction pattern at 1.55 μm. (a) Far field intensity. (b) Near field intensity. (c) Far field $|E_y|^2$. (d) Near field $|E_y|^2$.

frequency components, but its magnitude is usually negligible. However, approaching the SPP frequency, the vectorial nature becomes more prominent (figure 4) (asymptotically at the

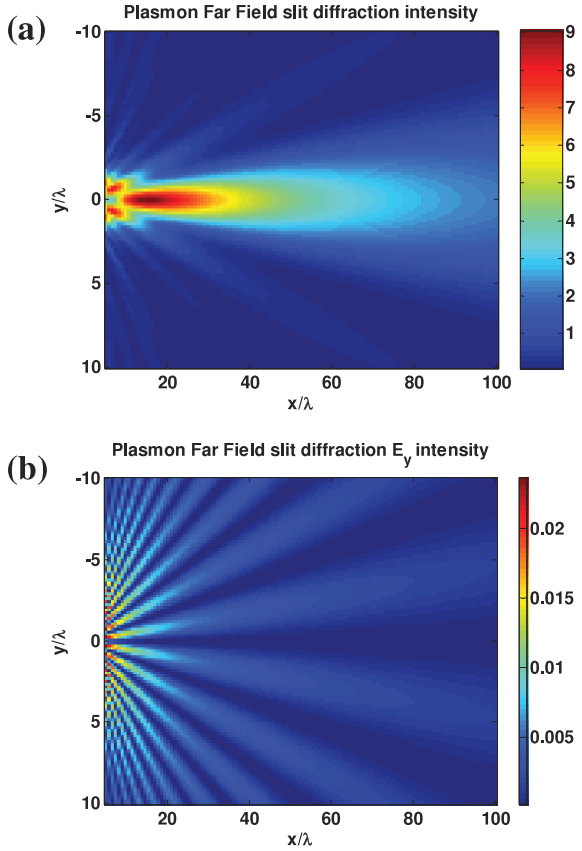

Figure 4. Single (4λ) slit SPP diffraction pattern at 413 nm. (a) Field intensity. (b) $|E_y|^2$.

SPP frequency both components are equal). The higher frequency longitudinal E_y component is important at such frequencies for proper design of plasmonic based circuitry. We compared the diffraction patterns calculated by our vectorial model and a scalar model which employs an effective index approach. Figure 5 represents the intensity profiles on a virtual screen, situated at a distance of 30 wavelengths from the slit. The profile was calculated by both techniques and at different wavelength excitations. Far from the surface plasmon resonance wavelength the SPP may be treated as an almost scalar wave (at least for diffraction related scenarios) (figure 5(a)); however, the vectorial nature turns out to be significant as the excitation wavelength approaches the surface resonance (figures 5(b) and (c)). The normalized relative error between the models was calculated at 1.55 μm as 2%, at 680 nm as 16% and at 413 nm as 58%. The visibility of the diffraction patterns is also different for vectorial and scalar models.

We used the results of the single-slit diffraction to construct a model for the Young's double-slit experiment by solving the configuration of the two slits, as depicted in figure 6(a). We used a layout very similar to the experimental set up reported in [17]: each slit is 2 μm wide and they are separated by a 4 μm screen. The results of a numerical experiment may be seen in figure 6(b).

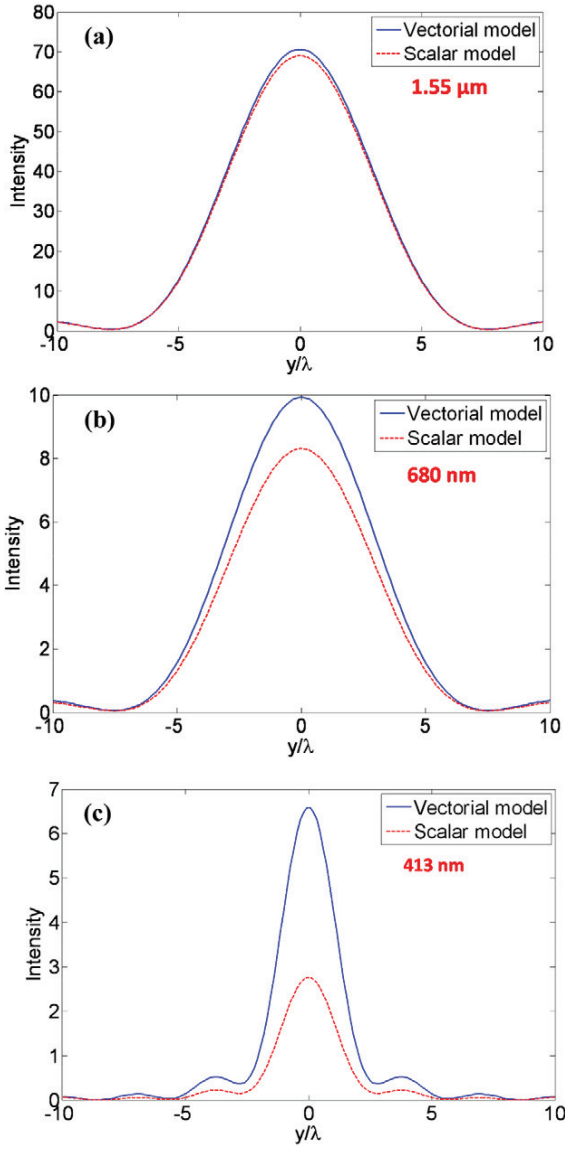

Figure 5. Single (4λ) slit SPP diffraction pattern profile at a distance of 30λ from the slit. Blue solid line, our vectorial model; red dashed line, scalar model. Excitation wavelength of: (a) 1.55 μm, (b) 680 nm and (c) 413 nm.

The results closely resemble the measurement results described in [17]—the high frequency features of the near field as well as the appearance of a main lobe are described by our full-vectorial model but are absent in the original scalar model employed in [17]. We compare the interference pattern profile at a distance of 15 wavelengths from the slits (figure 6(c)) and estimated the relative deviation of the results to be as high as 16%.

5. Conclusions

We investigated a full-vectorial point source for surface plasmon modes, showing it is suitable for a proper description of two-dimensional diffraction problems. The diffraction from

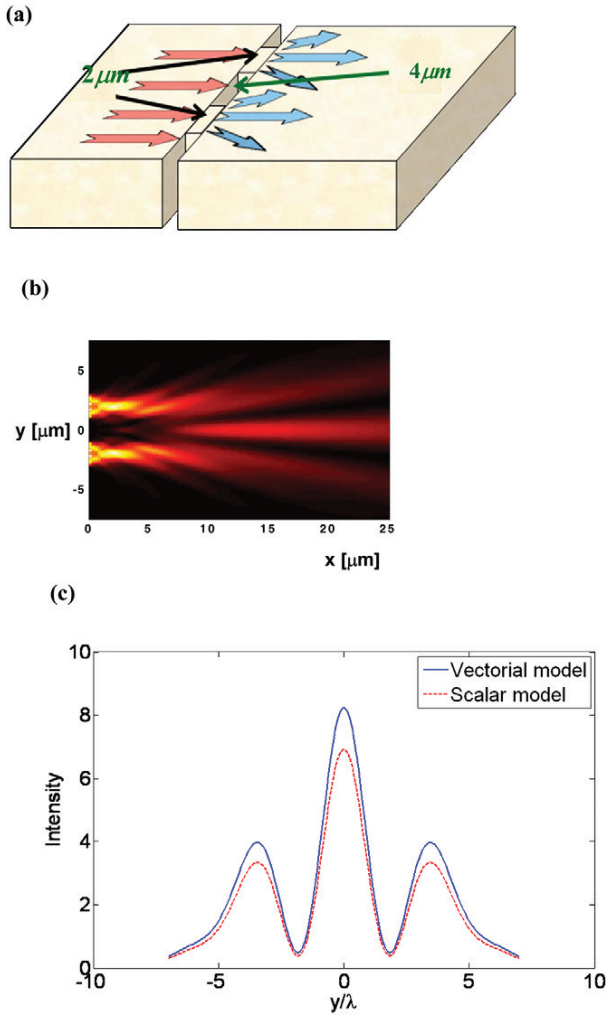

Figure 6. SPP Young's double-slit experiment. (a) Basic configuration. (b) Field intensity estimated by our full-vectorial model for comparison with experimental and theoretical data [17]. (c) Interference pattern at a distance of 15 wavelengths from the slits. Blue solid line, vectorial model; red dashed line, scalar model.

a single slit was obtained with delicate near field features. The investigated model was compared to a widely used scalar one, based on the effective index approach. The deviations between the models turns out to be very large near the surface plasmon resonance, where the transverse and longitudinal components of the plasmonic modes are comparable and the vectorial nature cannot be discarded. Results of a plasmonic double-slit experiment were shown to be in very good correlation between existing measurements and our model, while the scalar model fails to show adequately the near field patterns and underestimates the overall intensity (and therefore the visibility) of the fringes.

References

[1] Raether H 1988 *Surface Plasmons on Smooth and Rough Surfaces and on Gratings* vol 111 (Berlin: Springer)

[2] Ozbay E 2006 Plasmonics: merging photonics and electronics at nanoscale dimensions *Science* **311** 189–93

[3] Ginzburg P, Arbel D and Orenstein M 2006 Gap plasmon polariton structure for very efficient microscale-to-nanoscale interfacing *Opt. Lett.* **31** 3288–90

[4] Ginzburg P and Orenstein M 2007 Plasmonic transmission lines: from micro to nano scale with $\lambda/4$ impedance matching *Opt. Express* **15** 6762–7

[5] Zheludev N I 2008 What diffraction limit? *Nat. Mater.* **7** 420–2

[6] Ozbay E and Aydin K 2008 Negative refraction and imaging beyond the diffraction limit by a two-dimensional left-handed metamaterial *Photon. Nanostruct.* **6** 108

[7] Burke J J, Stegeman G I and Tamir T 1986 Surface-polariton-like waves guided by thin, lossy metal films *Phys. Rev.* B **33** 5186–201

[8] Bozhevolnyi S I, Volkov V S, Devaux E, Laluet J-Y and Ebbesen T W 2006 Channel plasmon subwavelength waveguide components including interferometers and ring resonators *Nature* **440** 508–11

[9] Satuby Y and Orenstein M 2007 Surface-plasmon-polariton modes in deep metallic trenches—measurement and analysis *Opt. Express* **15** 4247–52

[10] Maier S A, Kik P G and Atwater H A 2002 Observation of coupled plasmon-polariton modes in Au nanoparticle chain waveguides of different lengths: estimation of waveguide loss *Appl. Phys. Lett.* **81** 1714

[11] Feigenbaum E and Orenstein M 2007 Optical 3D cavity modes below the diffraction-limit using slow-wave surface-plasmon-polaritons *Opt. Express* **15** 2607–12

[12] Barnes W L, Dereux A and Ebbesen T W 2003 Surface plasmon subwavelength optics *Nature* **424** 824–30

[13] Ditlbacher H, Krenn J R, Schider G, Leitner A and Aussenegg F R 2002 Two-dimensional optics with surface plasmon polaritons *Appl. Phys. Lett.* **81** 1762–4

[14] Liu Z, Steele J M, Srituravanich W, Pikus Y, Sun C and Zhang X 2005 Focusing surface plasmons with a plasmonic lens *Nano Lett.* **5** 1726–9

[15] Radko I P, Bozhevolnyi S I, Evlyukhin A B and Boltasseva A 2007 Surface plasmon polariton beam focusing with parabolic nanoparticle chains *Opt. Express* **15** 6576–82
Beermann J, Radko I P, Boltasseva A and Bozhevolnyi S I 2007 Localized field enhancements in fractal shaped periodic metal nanostructures *Opt. Express* **15** 15234–41

[16] Yin L, Vlasko-Vlasov V K, Pearson J, Hiller J M, Hua J, Welp U, Brown D E and Kimball C W 2005 Subwavelength focusing and guiding of surface plasmons *Nano Lett.* **5** 1399–402

[17] Zia R and Brongersma M L 2007 Surface plasmon polariton analogue to Young's double-slit experiment *Nat. Nanotechnol.* **2** 426–9

[18] Ebbesen T W, Lezec H J, Ghaemi H F, Thio T and Wolff P A 1998 Extraordinary optical transmission through sub-wavelength hole arrays *Nature* **391** 667–9

[19] Huang F M, Kao T S, Fedotov V A, Chen Y and Zheludev N I 2008 Nanohole array as a lens *Nano Lett.* **8** 2469–72

[20] Sanchez-Gil J and Maradudin A 2004 Dynamic near-field calculations of surface-plasmon polariton pulses resonantly scattered at sub-micron metal defects *Opt. Express* **12** 883–94
Sánchez-Gil J and Maradudin A 1999 Near-field and far-field scattering of surface plasmon polaritons by one-dimensional surface defects *Phys. Rev.* B **60** 8359

[21] Goodman J W 1988 *Introduction to Fourier Optics* 2nd edn (New York: McGraw-Hill)

[22] Chang S, Gray S and Schatz G 2005 Surface plasmon generation and light transmission by isolated nanoholes and arrays of nanoholes in thin metal films *Opt. Express* **13** 3150–65